 DOI: 10.35382/TVUJS.14.3.2024.4

# OPTIMIZATION OF AUTOMATED PRODUCTION LINE FOR NANO-COATED FILTER MEDIA

Tay Kay Vooi[1], Lim Joo Eng[2*], Mum Wai Yip[3], Choon Lih Hoo[4], Prabhu Rajamamundi[5]

**Abstract** – *Nano-coated filters is crucial in preventing the spread of airborne viruses like COVID-19, influenza, and other respiratory viruses. Nano-coatings with antiviral properties significantly enhance the filter's ability to capture and deactivate these pathogens, providing essential protection in high-risk environments such as hospitals, public transportation, and indoor spaces. This study focuses on developing a streamlined production system that integrates nano-coating directly onto filter media fabrics, addressing inefficiencies and high costs associated with the current separate nano-coating process. The proposed system features four process stations: unwinding the fabric, spraying nano-liquid, drying, and rewinding the fabric. The integrated system ensures uniform application of the nano-coating through rollers and fine atomisation nozzles. The drying process using infrared radiation and heated air with thermocouples provides even heating and effective bonding of the coating. The rewinding process, supported by web guiding, load cells, and feedback signals, maintains proper fabric alignment and tension, ensuring accurate spooling. The cast iron EN9-made structure supports filter materials ranging from 5 kg to 9 kg in weight. The system is powered by a servo motor with 31.75 Nm torque and speed of 111.4 revolution/minute, and a pump operates at 60 psi with 4.4 $\times$ $10^{-7}$ $m^3/s$ flowrate and 6.7 W power. The 13.5 kW curing oven maintains a temperature range of 75$^o$C–80$^o$C for 45 seconds. The automation and integration of these processes into a single continuous production line contribute to the development of more efficient, scalable production methods, and enhance the consistency of producing high-quality filtration materials.*

***Keywords: airborne micro-droplet, antiviral filter, infrared, integrated production line for nano-coated filter, roll-to-roll web, spray-dried.***

## I. INTRODUCTION

Air filters are simple, flexible devices that clean the air by trapping particles, including airborne viruses. Filter media varies based on the application and efficiency requirements, with common materials including fiberglass, used in high-efficiency particulate air (HEPA) filters for small particles and volatile organic compound (VOC) removal, as well as polyester, polypropylene, cellulose, and nylon. Research shows that hydrophobic nanoparticle coatings can block water-based micro-droplets carrying viruses [1]. Studies in New York City have proven their effectiveness in capturing COVID-19 droplets without affecting airflow [2, 3]. Nano-coated filters improve filtration efficiency by capturing ultrafine particles, including viruses and bacteria. The coating enhances performance, preventing fouling and resisting microbial growth. It also adds antimicrobial properties and durability, making it ideal for air purification, water treatment, and biomedical devices [4–10]. This research collaborates with a company specializing in filter manufacturing and innovation. The company, which produces fiberglass, polyester, nylon, and HEPA filters, plans to launch nano-coated filters in response to the high demand caused by

[1,2,3]Tunku Abdul Rahman University of Management and Technology, Malaysia
[4]Sunway University, Malaysia
[5]Anna University, Chennai, India
*Corresponding author: limje@tarc.edu.my
Received date: 18$^{th}$ July 2024; Revised date: 17$^{th}$ September 2024; Accepted date: 30$^{th}$ September 2024

COVID-19, without needing major facility upgrades. The nano-coating process involves spraying with nano-liquid, followed by curing. The necessary steps are unwinding, spraying, curing, and rewinding the filter media. The aim is to design an integrated production line with these four stations, customized to meet the company's needs and facilitate industry adoption. Success will provide the company with a system for manufacturing nano-coated filters. Implementing these filters in heating, ventilation, and air-conditioning (HVAC) systems will significantly reduce the risk of virus exposure, including COVID-19. Additionally, nano-coated filters will enhance the performance of face masks and respiratory devices.

## II. LITERATURE REVIEW

A critical analysis of previous research on the development and application of nanotechnology in manufacturing, specifically in the production of spray-dried nanoparticles on substrates, primarily focuses on the development and evaluation of effective nano-coatings. However, most studies do not address the integrating of nano-coating applications within an industrial production line [11–14]. Typically, the processes of coating, drying, and curing are carried out manually in multiple stages, which increases the risk of contamination, inconsistencies in coating thickness, and production delays. Although nano-spray drying technology has proven effective for nanoparticle production, future studies must address the commercial demands of industrial-scale production [11]. Research highlights the potential of nano spray drying in manufacturing polymeric nanoparticles, but scaling up this process remains challenging [14]. The development of fully integrated systems including workpiece handling, in-process sensing, and control mechanisms, will enhance the practical applications of nano-manufacturing [14]. This study aims to address these gaps by employing roll-to-roll (R2R) manufacturing technology to design and integrate a production line for nano-coated fabric filters. Streamlining the process into a single, continuous production line will directly respond to the need for more efficient and scalable production methods.

### *A. Web roll-to-roll system and theories*

Web R2R technology applies to manufacturing processes that involve roller-transported material such as papers, films, foils, fabrics, nonwovens, textiles, or any thin, continuous material. It is a cost-effective mass-production method commonly used in industries like textile printing, packaging, electronics, and adhesive tapes. The process involves a continuous roll or strip of flexible material, called a web, that moves through rollers for various operations. In a typical setup, as shown in Figure 1, the web is unwound, processed through several steps depending on the application requirements, and then rewound onto the coil.

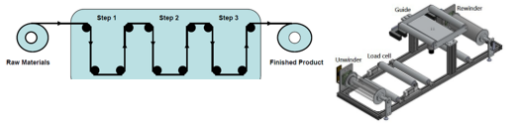


Fig. 1: Typical R2R setup and its system components (R2R manufacturing for flexible display)

The R2R systems consist of several subsystems: the unwinder unit, load cell unit, guide unit, and rewinder unit. The unwinder unit unwinds the web material and provides pulling tension from the rewinder unit. The load cell unit provides constant tension feedback. The guide unit guides and corrects the web's lateral motion. Finally, the rewinder unit rewinds the web material into a coil. The system typically involves placing the web onto an unwind roll, with reverse tension often coupled to a motor or friction belt. Passive rollers monitor tension and speed while dampening [15, 16]. Key components include a guide mechanism, actuator (brakes and motors), sensors, a web tension detector, and a controller, as shown in Figure 2. The guide mechanism moves the web, positioned at different locations of a R2R machine that requires web alignment,

and terminal web guides are used at the machine entry or exit points [17–20]. The unwinder is supported at both ends to reduce bending. A ball bearing inside the supporter allows shaft rotation, while passive coil guides prevent excess lateral motion. Guides have set screws to fix their position on the shaft, and the inner sides fit through the coil to secure and unwind it. A housing bolted to the back plate enables rotation, and a shaft coupling connects the shaft to the brake, with the brake housing supporting the shaft. The rewinder unit such as the unwinder, consists of a supporter, coil guide, and back plate. It uses a torque motor to maintain constant tension during rewinding, with a motor coupling connecting the torque motor to the shaft.

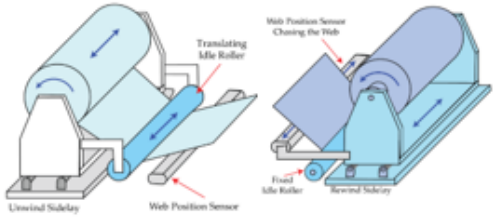


Fig. 2: A web guide at unwinding and rewinding side (R2R technologies)

### *B. Basis web handling principles*

Web handling requires precision to prevent lateral motion, wrinkling, and breakage. Web guides align the material perpendicularly to the roller's axis according to the 'Normal entry law', see Figure 3.

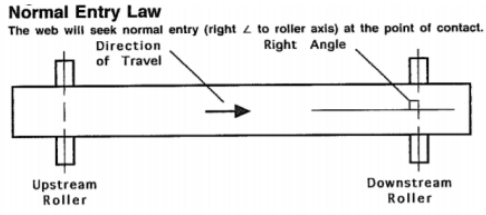


Fig. 3: Principles of 'Normal entry law' (R2R technologies)

Additionally, tension, nip, and torque (TNT) are key winding concepts used to optimize roll structure, ensuring correct hardness and without flaw. Tension, regulated by surface drive, manages the winding web for slitting and spreading. Nip, controlled by lay-on roll loading, pertains to the pressure rolls, while torque, generated by the center drive (or torque drum), influences the roll's internal structure [18, 21].

**Rollers**

Rollers are essential in R2R systems for moving web material. They can be cylindrical or chamfered to influence web behaviour. They impact machine performance by changing the web's path, tension, and wrinkle risk. The number of rollers depends on the unsupported span of the web, which varies with its width and thickness. Too long a span can cause sagging or vibration, while too short can lead to alignment issues. Proper roller sizing follows the specific formula that recommends a length-to-diameter ratio roller not exceeding 16 [22], see Equation (1), where R is the ratio value, L is roller length, D is the roller diameter.

$$R = \frac{L}{D} \qquad (1)$$

**Unwind, rewind and control**

The raw web is unwound from a coil, processed, and then rewound into a coil for inventory. The main winding types are centered surface and turret wind. Turret winding is useful for soft rolls like webs and films. It consists of two center winds with a pivot for dual directions winding and can index an empty core into place once the previous roll is finished for continuous operation [18, 23–26], as shown in Figure 4.

**Web guides and position control**

Lateral motion is managed with web guides to keep the web and roller aligned. There are two main types: passive and active guides. Passive guides, like edge and surface guides, use mechanical isolation to control the web's lateral movement. Active guides, such as displacement and steering guides, use servo actuators based on sensor measurement to actively keep the web centered [18, 23–26], as shown in Figure 5.

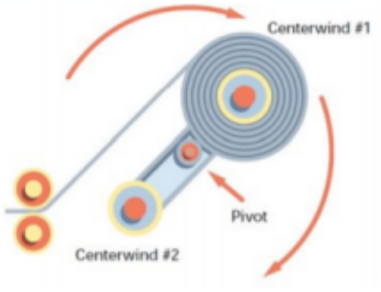


Fig. 4: Turret centre winding [23]

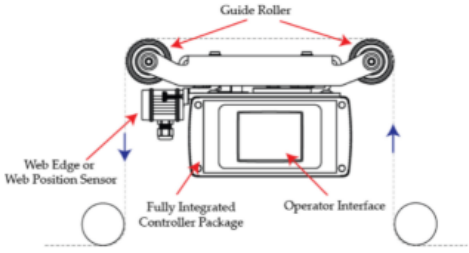


Fig. 5: Guide mechanism [25]

The winding process is key to production speed as it controls the pulling resistance on the web. The material's line speed isn't equal to the winding motor's rpm. As the material winds and the coil diameter increases, keeping the motor's rpm constant will increase surface speed. To keep line speed constant, the winding motor must adjust speed as the coil diameter changes, showing an inverse relationship between the motor's rpm and coil radius. Most processes need constant line speed during steady running, requiring a winding controller with linear velocity matching. Maintaining constant web tension is also necessary. Tension equals torque divided by coil radius, so if tension is constant, torque must increase as the radius increases. The winder motor can be controlled to regulate fixed current and provide enough torque as the coil radius increases, thus maintaining constant tension. An unwind side lay (simple, moves roll) or displacement guide (complex, small actuators, no roll movement) was used to correct offset layers. displacement guides (easy, compact) or steering guides (best for large spans) were used for intermediate processing. A winder side lay guide (easiest) or a displacement guide before the winder was used for winding [27].

**Web tension and control**

Web tension is the force applied along the length of the web material, measured as force per unit width. There are three main control zones: unwind, process (nip), and rewind, each with different tension control needs. The goal is to keep tension steady and below the web's elastic limit to avoid damage. As a roll's diameter changes, torque must be adjusted to maintain proper tension, which is typically managed by adjusting torque relative to the roll diameter [28–30], see Figure 6. Three common mechanisms for measuring web tension are the dancer, load cell, and accumulator. Load cells are applicable, it uses sensors to convert tension into an electrical signal. It often includes a strain gauge in a Wheatstone bridge, which changes resistance when force is applied. This change is measured and converted into a signal that the controller uses to adjust the winding speed and keep the tension constant within 10% of the set point [23, 28, 31–33].

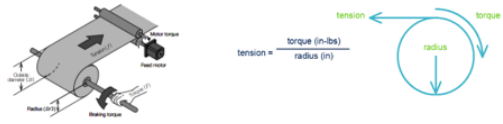


Fig. 6: Web tension and formula (Web Tension Control Basics)

**Motor**

A direct current (DC) servo motor delivers controlled speed and position. Servo motors maintain consistent tension by adjusting torque based on reel diameter. While vector control inverters offer more stable rotational speed and smoother torque transitions, they may be less accurate than alternating current (AC) servo motors. Equations (2) to (4) are used to determine the size of the motor with the maximum and minimum torque ($T$) in Nm, tension ($F$) in N,

and web diameter ($D$) in m. The maximum and minimum rotational speed ($N$) in rpm, line speed ($V$) in m/s, and the motor capacity ($P$) in W.

$$T_{max} = \frac{D_{max}}{2} x\ F_{max}; T_{min} = \frac{D_{min}}{2} x F_{min} \quad (2)$$

$$N_{max} = \frac{V_{max}}{\pi\ x\ D_{min}}; N_{min} = \frac{V_{min}}{\pi\ x\ D_{max}} \quad (3)$$

$$P = \frac{0{,}0167 F_{max} V_{max}}{D_{max}} \quad (4)$$

**Brakes/clutches**

Air brakes use compressed air to operate drum or disc brakes or both. It uses air to push a friction plate, providing higher torque and heat capacity and making it ideal for winding and unwinding applications. An electro-pneumatic converter can be used to drive a tension controller as shown in Figure 7 [34]. Equations (3) to (4) are also used for selection of brakes.

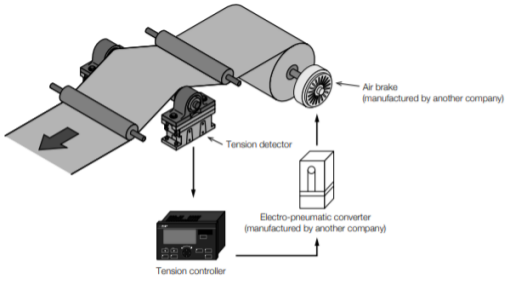


Fig. 7: Air brakes [34]

*C. Spraying/coating technologies*

Solution-based methods are used to deposit nanomaterials onto a substrate for films of varying thicknesses, by layer-by-layer deposition. Spray coating is popular for its simplicity and low cost. In this method, nanoparticles are sprayed onto a substrate to create transparent films at room temperature. Nanoparticles are dispersed in the matrix at the nanoscale, achieving coatings typically under 100 nm thick. The nanomaterial mass fraction ranges from 3% to 7% [35]. After application, the coating often undergoes curing. To achieve high-quality spray performance, selecting the appropriate spray nozzle and flow control equipment like a pump is essential. A complete spraying system typically includes nozzles, pipes, valves, pressure regulators, filters, pumps, control valves, sensors, variable frequency drives (VFDs), switches, relays, electrical hardware, and a structural frame [36]. Uniform coating on fabric is achieved by producing even spray lines along the target areas, considering spray angle and nozzle spacing. Flat fan nozzles may not be perfect even due to soft pattern edges and a tapering effect, resulting in lower spray distribution. To compensate, sprays can be overlapped to ensure a more equal coating. However, care must be taken to avoid collision between overlapping sprays, which can cause droplet agglomeration and reduced uniformity. Therefore, it is common to slant each spray nozzle to prevent contact between sprays [37]. Whereas spray coverage is the area a nozzle covered at a specific location, determined by the nozzle's spray angle and the distance between the nozzle to the material [37]. It is influenced by five variables: spray angle (A), actual spray coverage (B), effective spray angle (C), distance from nozzle/height (D), and theoretical spray coverage (E), as shown in Figure 8.

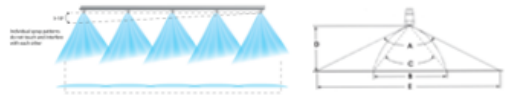

Fig. 8: Slanted position [33] & spray coverage [36]

Nozzles are either hydraulic or air atomising, with air atomising nozzles available in siphon-fed, external mix, and internal mix designs. Full cone and mist patterns are suitable for even coating and consistently without exerting high pressure onto the web [36]. A summary of the description is shown in Table 1.

The high-volume low-pressure spray gun, suitable for dispersing nanomaterials onto fabric, operates within a limited air pressure range to achieve low velocity patterns, good finish, and high transfer efficiency [38]. It uses a liquid

Table 1: Spray pattern types

| Spray pattern | Description |
|---|---|
| Full Cone  | Provide uniform fluid coverage over a specific area but quickly turns to mist. The nozzles aim to maintain the full cone pattern as long as possible. |
| Mist  | Spray patterns become mist, used for cooling, moistening, or humidifying, with mist nozzles creating small droplets at low flow velocity. |

pressure feed tank for medium to large-scale jobs, with air pressure for atomisation and the fluid amount is controlled by a regulator at the air source.

**Pump power**

Equation (5) to Equation (12) are used to calculate the required power for pumping and spraying the nanoparticles liquid onto the filter [39].

a) Volumetric flow rate:

$$Q(m^3/s) = AU \qquad (5)$$

where $A$ is the nozzle cross-sectional area ($m^2$) and $U$ is the flow velocity (m/s)

b) Reynold number:

$$e = \rho U d/\mu \qquad (6)$$

where $\rho$ is the fluid density (kg/$m^3$), $U$ is the fluid velocity (m/s), $d$ is the pipe diameter (m) and $\mu$ is the dynamic viscosity of the fluid (N/$m^2$).

c) Darcy friction factor, a dimensionless term for the friction loss due to fluid flow in a pipe is,

+ For laminar flow:

$$f = 16/Re \qquad (7)$$

+ For turbulent flow:

$$f = 0.079 \,/\, Re^{¼} \qquad (8)$$

d) Headloss in a pipeline:

$$h_f(m) = (4fl/d)(U^2/2g) \qquad (9)$$

where $d$ is the pipe diameter (m), $l$ is the pipe length (m), $U$ is the fluid velocity (m/s) and $g$ is the gravity acceleration (m/$s^2$).

e) With $K$ as the loss coefficient, the losses due to pipe fitting and bends,

$$h_f = K(U^2/2g) \qquad (10)$$

f) Bernoulli equation:

$$\frac{P_1}{\rho g} + \frac{U_1^2}{2g} + Z_1 = \frac{P_2}{\rho g} + \frac{U_2^2}{2g} + Z_2 + \sum h_f \qquad (11)$$

where d is for pressure (Pa), $\rho$ is the density of the fluid (kg/$m^3$), $Z$ is the height of the fluid level (m), $U1$ and $U2$ are the initial and final fluid velocity (m/s).

g) Pump power required:

$$P = \rho g h_f Q \qquad (12)$$

*D. Curing technologies for nano-liquid coating*

The infrared ray method effectively cures nanoparticles on filters using heaters set at 75–80$^o$C. The drying area has aluminium-covered inner walls to deflect infrared radiation and asbestos-insulated outer walls. Ceramic heaters, which emit long-wave infrared radiation, are commonly used for various applications, including curing, thermoforming, and drying.

**Power input for infrared ray heater**

The heat input parameter is determined using the thermodynamic equilibrium approach, ensuring that the heat emitted by the radiators, Q in Joule, equals the total heat received and lost by the material and chamber walls over time, as detailed in Equations (13) to (19) [40].

$$Q = Q_1 + Q_2 + Q_3 + Q_4 \qquad (13)$$

where $Q$ is the total amount of heat energy of the system, $Q_1$ is the heat absorbed by the material, $Q_2$ is the heat absorbed for evaporation of liquid, $Q_3$ is the heat absorbed by water vapour for heating the chamber and $Q_4$ is heat lost from walls of the heater.

$$Q_1 = \Sigma(G_{1i} C_{1i} \triangle t) \qquad (14)$$

where $G_{1i}$ is the mass flow rate of the filter (kg/hr), $C_{1i}$ is the specific heat of the filter

(J/kg$^o$C) and $\triangle t$ is the temperature difference of filter before and after drying [38].

$$G_1 i = vw(m/A_f) \qquad (15)$$

where $v$ is line speed (m/s), $W$ is the filter width (m), $m$ is filter mass (kg) and $A_f$ is the area of the filter ($m^2$).

$$Q_2 = \Sigma G_2 q' \qquad (16)$$

$G2$ is the mass flow rate of evaporated liquid (kg/hr) and $q'$ is heat of vaporization liquid (J/kg$^o$C).

$$Q_3 = G_2 C_3 \triangle t_3 \qquad (17)$$

where $C_3$ is specific heat water vapour (J/kg$^o$C) and $\triangle_{t_3}$ is temperature difference of the water vapour from 100$^o$C to the heater temperature ($^o$C).

$$Q_4 = h_c A(t_2 - t_1)^{1.25} + 5.67x10^{-8} Ae[(T_1)^4 - (T_2)^4] \qquad (18)$$

where $h_c$ is convective heat transfer coefficient (W/$m^2 \cdot ^o$C), $A$ is the total outer surface area ($m^2$), $t_1$ is surrounding temperature, $e$ is emissivity of the heater, $t_2$ is atmosphere temperature inside the heater, $T_1$ absolute temperature of surrounding and $T_2$ absolute temperature of atmosphere temperature inside the heater. $T$ unit is ($^o$C).

Finally, the heater power

$$P = QK_2/3600K_1 \qquad (19)$$

where $K_1$ is the voltage fluctuations correction coefficient and $K_2$ is power reserve coefficient.

## III. RESEARCH METHODS

### A. Web coil and nano-solution specification

Table 2 lists the web material and nano-liquid specified by industry requirements.

Table 2: Web coil and nano-liquid requirements

| Material | Description | Material | Description |
|---|---|---|---|
| Web material | Thermal bonded polyester fibre, thickness from 8 mm to 25 mm. | Nano-liquid viscosity | Similar to water |
| Filter roll size | Diameter 2 m x length 20 m | Curing temperature | 75°C to 80°C for 45 s |
| Filter roll weight | For 8 mm fibre, weight is 5 to 6 kg For 25 mm fibre, weight is 8 to 9 kg | Nano-liquid usage | 1,000 ml for 150 m$^2$ filter area |

### B. Working principles of the system

The fabric roll is first fed through a series of rollers that adjust its position and tension, ensuring it spread out evenly without wrinkles. At the spraying station, a system of nozzles applies a finely atomise nano-coating onto the fabric surface, with the amount and distribution of the spray-controlled to ensure uniform coverage. Next, the coated fabric enters a curing oven, where it is exposed to controlled heat through a combination of infrared radiation and heated air. Finally, the cured fabric is wound back into spools, using the same roller mechanism as in the first station to ensure the fabric is wound evenly.

### C. Design calculations

**Web roller diameter**

For a required roller length of 1.6 m, the roller diameter, D should be 0.1 m or less.

$$D = \frac{1.6}{1.6} = 0.1m \qquad (20)$$

**Motor sizing**

The force $F$ ranges from 50 N to 100 N, the web diameter ranges from 0.01 m to 0.635 m, and the line speed ranges from 1.0 m/min to 3.5 m/min. Using Equation (2) to Equation (4), the maximum $T_{max}$ and minimum torque $T_{min}$ are 31.75 Nm and 0.25 Nm, respectively. The corresponding maximum and minimum rotational speed are $N_{max}$ = 111.41 rpm and $N_{min}$ = 0.5 rpm.

The power requirement is calculated using the following Equation (21).

$$P = \frac{0.0167\,(100)(3.5)(0.635)}{0.01} = 371.16\,W \qquad (21)$$

Hence, the motor selection will be based on the computed result.

**Brake sizing**

With the same approach, the following parameters can be round, $T_{max}$ = 31.75 Nm, $T_{min}$ = 0.25 Nm, $N_{max}$ = 111.41 rpm, $N_{min}$ = 0.5 rpm and $P$ = 5.845 W. This leads to the brake selection.

**Pump power**

For every 150 $m^2$ of filter area, it requires a nano-liquid of 1,000 ml. For a roll of 1.2 m width, every meter length requires $8 \times 10^{-6}$ $m^3$ amount of nano liquid. With this amount of nano liquid and $4.416 \times 10^{-7}$ $m^3$ of nano required per second, the line speed v $\sim$ 3.5 m/min. For 45 s of curing time, the heat zone length, L $\sim$ 2.5 m.

Using Equations (5) to (12), for a nozzle diameter 0.0762 mm, fluid velocity is,

$$V = \frac{Q}{A} = \frac{4.416\times10^{-7}}{\pi(0.0762)^2} = 24.2\ m/s \quad (22)$$

$$Re = \frac{\rho u d}{\mu} = \frac{998.2(24.2)(0.0531)}{1.002x10^{-3}} = 1.28x10^6 \text{ (turbulent flow)} \quad (23)$$

$$f = \frac{0.079}{Re^{\frac{1}{4}}} = \frac{0.079}{(1.28x10^6)^{\frac{1}{4}}} = 2.35x10^{-3} \quad (24)$$

From Bernoulli Equation (25);

$$\sum h_f = \frac{\frac{2(4)(2.35x10^{-3})(0.225)}{0.0531} + 0.9 + 2(25)}{2(9.81)} + \frac{\frac{4(2.35x10^{-3})(0.15)}{0.0283} + \frac{4(2.35x10^{-3})(1.68)}{0.0283}}{2(9.81)} x24.2^2 \quad (25)$$

Hence, the pressure, $P1$ is $17.6 \times 10^3$ kPa while the power is as Equation (26).

$$P = \rho g h_f Q = 998.2(9.81)(1539.66)(4.416 \times 10^{-7}) = 6.66\ W \quad (26)$$

The design constants and assumptions used for the above calculations are: 1) Pipes are assumed to be smooth; 2) Pump origin height set at 0 m; 3) Fluid has similar properties as water; 4) Initial fluid velocity is 0 m/s; 5) Density of the fluid is same as water; 6) Dynamic viscosity of the fluid is $1.002 \times 10^{-3}$ kg/ms; 7) The inner diameter of the larger pipe is 53.1 mm; 8) Larger pipe length is 275 mm; 9) The inner diameter of the small pipe is 28.3 mm; 10) Smaller pipe 1, length is 150 mm; 11) Smaller pipe 2, length is 1600 mm; 12) Loss coefficient of 90$^o$C elbow is 0.9; 13) Loss coefficient of the valve is 50.

Selecting the spray nozzle with the lowest specifications reduces power requirements, eliminating the need for a longer infrared ray heater due to higher nano-liquid flow rate. As a result, the pump pressure is about 17.6 $\times$ 103 kPa, and the required power is 6.66 W.

**Infrared ray heater power**

For infrared ray heater power calculation, the total heat energy needed includes the sum of four components: 1) heat absorbed by filter (Q1); 2) heat absorbed for evaporation of coating (Q2); 3) heat absorbed by water vapor for chamber heating (Q3); and 4) heat lost from walls of chamber (Q4). Using Equations (13) to (19), filter mass enters to heater zone per hour, $G_{1i}$, is

$$G_{1i} = (3.5\ m/min \times 60)1.2\ m \times (7\ kg\ /\ 1.2\ m \times 20\ m) = 73.5\ kg/\ hour \quad (27)$$

$$Q_1 = 73.5 \times 0.97 \times (80 - 25) = 3921.23\ kJ/h \quad (28)$$

$$\sum G_2 = 4.416 \times 10^{-7}\ m^3/s = 1.59\ kg/h \quad (29)$$

$$Q_2 = 1.59(2536) = 4032.24\ kJ/h \quad (30)$$

$$Q_3 = G_2 C_3 \Delta t_3 = 1.59 \times 1.996 \times (100 - 80) = 63.47\ kg/h \quad (31)$$

$$Q_4 = 10(11.65)(80 - 25)^{1.25} + 5.67(10^{-8})(11.65)(0.1)[(353)^4 - (298)^4] = 17954.1\ kJ/h \quad (32)$$

Thus, the total heat energy required $Q$ and the minimum power for heater $P_{heater}$ to maintain its required temperature is 25971.05 kJ/h and 13.5 kW, respectively. A factor of 1.25 is accounted for uncovered areas losses and the infrared source efficiency. The design constants and assumptions [41–44] are $C_{1i}$ = 0.97 J/g$^o$C, $C_{1i}$ = 2536 kJ/kg$^{-1}$, $C_3$ = 1.996 kJ/kgK, $h_c$= 10 $m^2$K, $e$ = 0.1, $A$ = 11.65 $m^2$, $K_1$ = 1, $K_2$ = 1.5, room temperature = 25.0$^o$C and boiling temperature of liquid = 100.0$^o$C.

## IV. RESULTS AND DISCUSSION

The 3D design, shown in Figure 9, includes four stations: spreading filter media, spraying nano-liquid, curing, and rolling up fabric. The system is about 5.8 m long, 3.70 m wide, and

1.4 m high, with a metal structure made from EN9 carbon steel alloy, known for its hardness and wear resistance.

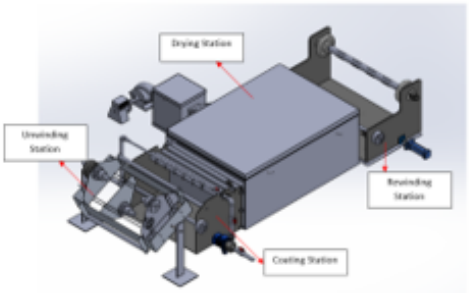


Fig. 9: 3D model of complete system

### A. *Station 1 'Unwinding station'*

The unwinder station is designed to unroll the filter. The 3D model is shown in Figure 10 and the main components are listed in Table 3.

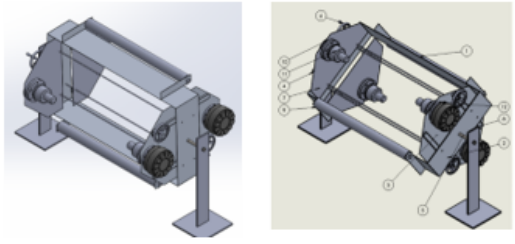

Fig. 10: Unwinding station

Table 3: Component list for Station 1

| No | Component | Qty | No | Component | Qty | No | Component | Qty |
|---|---|---|---|---|---|---|---|---|
| 1 | Unwinder frame | 1 | 5 | Rotational rod | 2 | 9 | Rollers | 2 |
| 2 | Linear rod | 4 | 6 | Handwheel | 4 | 10 | Connectors | 8 |
| 3 | Locking plate 1 | 2 | 7 | Support stand 1 | 1 | 11 | Hydraulic chuck | 4 |
| 4 | Locking plate 2 | 2 | 8 | Support stand 2 | 1 | 12 | Pneumatic brake | 2 |

The unwinder includes two pneumatic brakes, a hydraulic chuck for positioning and locking filter. The frame, with a linear motion rod, provides rotating capability and allows continuous loading of filter rolls. It features a locking plate and handwheel for adjusting to different filter widths for its flexibility for different filter width dimensions.

### B. *Station 2 'Coating station'*

At this station, the filter is coated with nano liquid sprayed by the nozzle located directly above the filter. Its 3D model is shown in Figure 11 and the main components are listed in Table 4.

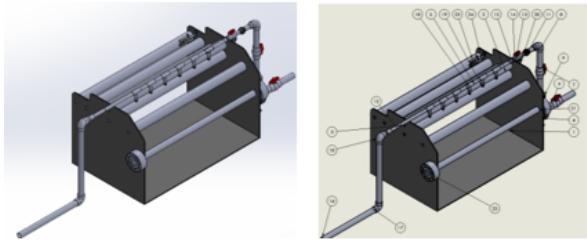

Fig. 11: Coating station

Table 4: Component list for Station 2

| No | Component | Qty | No | Component | Qty | No | Component | Qty |
|---|---|---|---|---|---|---|---|---|
| 1 | Spray frame | 1 | 9 | Union 2" | 1 | 17 | Elbow 2 | 1 |
| 2 | Rollers | 6 | 10 | Elbow 1 | 2 | 18 | Faucet socket, 15 mm | 6 |
| 3 | Pipe1, 25 mm | 1 | 11 | Union 1" | 1 | 19 | PJ nozzle | 6 |
| 4 | Water pump | 1 | 12 | Pipe3, 25 mm | 2 | 20 | Servo motor | 1 |
| 5 | Reducing Tee | 6 | 13 | Ball valve, 25 mm | 1 | 21 | Roller (T control) | 1 |
| 6 | Valve socket, 50 mm | 2 | 14 | Faucet socket, 25 mm | 1 | 22 | Load cell | 2 |
| 7 | Ball valve, 20 mm | 2 | 15 | Valve socket, 25 mm | 1 | 23 | Ultrasonic edge sensor | 1 |
| 8 | Pipe2, 50 mm | 3 | 16 | Pipe4, 50 mm | 2 | 24 | U bracket | 1 |

The 'PJ (pilot jet) Fine Atomisation Nozzle' is chosen with the following specifications: 20.3 cm coverage, $90^o$ spraying angle, mist spray pattern, 60 psi minimum pressure, and $4.416 \times 10^{-7}$ $m^3$/s minimum flow rate. Figure 12 shows spraying coverage with the nozzle positioned at $10^o$ slant to achieve an even and consistent coating [34].

Once the operator starts the automated spraying system, the nanofluid is pumped in and the spraying process begins. The filter, fed from the 'Unwinding station', is positioned and guided through the nozzle area by a motorized roller

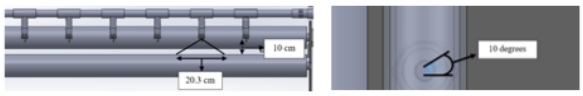


Fig. 12: Spray coverage and nozzle position

and monitored by a web tension load cell. The motor then guides the filter to the 'drying station', where an ultrasonic edge sensor detects and corrects the filter's alignment using a linear bearing system at the 'rewinder station'. Figure 13 shows the sensor positioning and the well-positioned rollers that guide the filter, respectively. The installed servo motor serves as the first driving unit of the line.

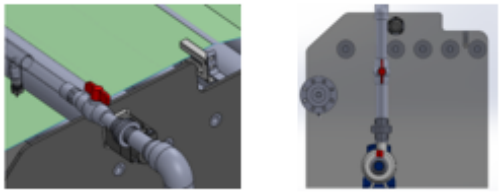

Fig. 13: Sensor position & roller position

### *C. Station 3 'Drying/Curing station'*

The filter is cured in this station using a hybrid infrared ray and heated air dryer. The 3D model of the design is shown in Figure 14 and the main components are listed in Table 5.

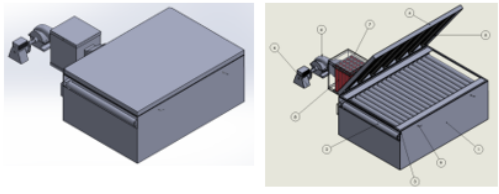

Fig. 14: Curing station

After the filter is coated, it enters the 'Drying station' which uses a hybrid infrared ray and heated air dryer to ensure even surface curing without overheating. Motorized conveyor rollers

Table 5: Component list for Station 3

| No | Component | Qty | No | Component | Qty | No | Component | Qty |
|---|---|---|---|---|---|---|---|---|
| 1 | Heater frame | 1 | 4 | Heater lid | 6 | 7 | Air heater frame | 1 |
| 2 | Conveyor rollers | 2 | 5 | Ceramic tube | 7 | 8 | Air heater tube | 1 |
| 3 | Thin section | 1 | 6 | Fan | 2 | 9 | Thermocouple | 1 |

move the filter through the heating process, with seven infrared ceramic bulbs spaced 30 cm apart. Thermocouples are placed at the beginning and end of the line ensure precise heat measurement, as shown in Figure 15. Heater air is blown into the infrared heater through six tunnels at the bottom, with the air heater temperature continuously monitored, as shown in Figure 16.

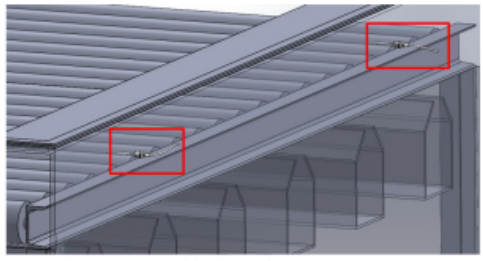

Fig. 15: Thermocouple position

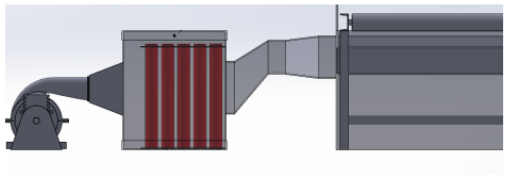

Fig. 16: Air heater with blower

### *D. Station 4 'Rewinding station'*

Figure 17 is the 3D model of the rewinding station and the main components are listed in Table 6.

The 'Rewinding station' rewinds the filter back to its original roll form after it exits the drying station. It uses an ultrasonic sensor and rollers equipped with web tension load cells to guide the filter on a core on the air-expanding shaft.

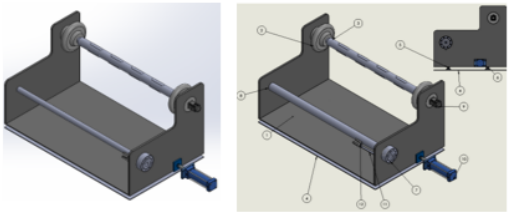

Fig. 17: Rewinding station

Table 6: Components list for Station 4

| No | Component | Qty | No | Component | Qty | No | Component | Qty |
|---|---|---|---|---|---|---|---|---|
| 1 | Rewinder frame | 1 | 5 | Linear rod | 6 | 9 | Servo motor | 1 |
| 2 | Safety chuck | 2 | 6 | Linear bearing | 6 | 10 | Hydraulic cylinder | 1 |
| 3 | Air shaft | 1 | 7 | Load cell | 2 | 11 | U bracket | 1 |
| 4 | Rewinder base | 1 | 8 | Rollers | 1 | 12 | Edge sensor | 1 |

The station includes a linear motion system with a 'shifting base' mechanism and two ultrasonic edge sensors for proper web alignment. These sensors provide feedback to a controller that adjusts alignment using linear bearing rods and motors. The servo motor serves as the second driving unit for the entire line. Figure 18 shows the linear bearing and its rod and sensor positioning.

Fig. 18: Linear bearing rod & sensor position

In summary, a model of the automated production line has been developed. The unwinding and rewinding stations use rollers to guide the filters. Load cells monitor web tension to control winding speed, and the filter's position is tracked for alignment adjustment at the rewinding station. The coating station uses fine atomisation nozzles for mist spraying. The drying station combines infrared heat and heated air for even drying, with thermocouples ensuring the right temperature is maintained.

## V. CONCLUSION AND RECOMMENDATIONS

Roll-to-roll technology is applied in designing the production line for the nano-coated filter media, which integrates four process stations: unwinding, coating, drying, and rewinding. The system is driven by a servo motor providing 31.75 Nm of torque at 111.4 rpm, while a pump operates at 60 psi with a flow rate of $4.4 \times 10^{-7}$ $m^3$/s and consumes 6.7 W of power. The curing oven, with a power requirement of 13.5 kW, maintains a temperature range of $75^oC$ to $80^oC$ for 45 seconds. Additionally, the metal plates for the system's structures are made from EN9, chosen for their strength and wear resistance to support various filter weights. The line operates continuously, moving the fabric smoothly through each station. Control systems, sensors, and feedback loops ensure a steady flow of material for efficient production and consistent product quality.

The project successfully delivers an optimal line design, improving production efficiency for nano-coated filters. Nano filters for air filtration can effectively protect society by reducing the risk of spread and exposure to viruses like COVID-19, influenza, and SARS-CoV. Moreover, nano filters are effective and reliable in various industries including water filtration and medical applications such as ventilators, respirators, and face masks, leading to improved safety, efficiency, and performance in their respective applications. For a broader impact, the production system promotes the practical application of nano-manufacturing for industrial-scale adoption.

Given the project's complexity, future research efforts are recommended. It is suggested to conduct engineering analysis and prototype testing. Computational static and dynamic analysis can assess the strength of the machine under static load and vibration, while CFD analysis can evaluate the spraying and curing performance. A prototype can be developed for small-scale experiments as proof of concept. Additionally, an economic feasibility or cost-benefit analysis should be considered for large-scale deployment.

## REFERENCES


[1] Jazie AA, Albaaji AJ, Abed SA. A review on recent trends of antiviral nanoparticles and airborne filters: special insight on COVID-19 virus. *Springer Nature*. 2021;14(11): 1811–1824.

[2] Pilkington B. *Nanotechnology filter coatings to combat the spread of coronavirus*. https://www.azonano.com/article.aspx?ArticleID=5564 [Accessed 2nd September 2024].

[3] Kever J. *Nanotech filter coating offers promise against Covid-19*. https://www.uh.edu/news-events/stories/2020/september-2020/09292020-curran-covid-filter.php [Accessed 2nd September 2024].

[4] Zhu Q, Chua MH, Ong PJ, Lee JJC, Chin KLO, Wang S, et al. Recent advances in nanotechnology-based functional coatings for the built environment. *Materials Today Advances*. 2022;15: 100270. https://doi.org/10.1016/j.mtadv.2022.100270.

[5] Kausar A. Polymer coating technology for high performance applications: fundamentals and advances. *Journal of Macromolecular Science, Part A*. 2018;55: 440–448. https://doi.org/10.1080/10601325.2018.1453266.

[6] Li Q, Hu Y, Zhang B. Hydrophilic ZnO nanoparticle-based antimicrobial coatings for sandstone heritage conservation. *ACS Publication*. 2021;4(12): 13908–13918. https://doi.org/10.1021/acsanm.1c03224.

[7] Imani SM, Ladouceur L, Marshall T, Maclachlan R, Soleymani L, Didar TF. Antimicrobial nanomaterials and coatings: current mechanisms and future perspectives to control the spread of viruses including SARS-CoV-2. *ACS Nano*. 2020;14(10): 12341–12369. https://doi.org/10.1021/acsnano.0c05937.

[8] Nasiol. *Effective filter protection with nano coatings*. https://www.nasiol.com/nanoblog/effective-filter-protection-with-nano-coatings/ [Accessed 3rd Septemper 2024].

[9] Coulson S. Plasma processing: Nano-coating enhances filtration media. *Filtration & Separation*. 2010;47(4): 34–36.

[10] Wang Z, Zhong R, Lai T, Chen T. Preparation of UV-curable nano-WO3 coating and its infrared shielding properties. *Nanomaterials*. 2022;12(21): 3920. https://doi.org/10.3390/nano12213920.

[11] Chopde S, Datir R, Deshmukh G, Dhotre A, Patil M. Nanoparticle formation by nanospray drying & its application in nanoencapsulation of food bioactive ingredients. *Journal of Agriculture and Food Research*. 2020;2: 100085. https://doi.org/10.1016/j.jafr.2020.100085.

[12] Strojewski D, Krupa A. Spray drying and nano spray drying as manufacturing methods of drug-loaded polymeric particles. *Polymers in Medicine*. 2022;52(2): 101–111.

[13] Shafiee S, Zarrebini M, Naghashzargar E, Semnani D. Antibacterial performance of nano polypropylene filter media containing Nano-$TiO_2$ and clay particles. *Journal of Nanoparticle Research*. 2015:17(407): 1–9. https://doi.org/10.1007/s11051-015-3195-y.

[14] Okoli JU, Briggs TA, Major IE. Application of nanotechnology in the manufacturing sector: a review. *Nigerian Journal of Technology*. 2013:32(3): 379–385.

[15] Williams B. *Roll-to-Roll processing: The basics*. https://www.montalvo.com/roll-to-roll-processing-basics/ [Accessed 3rd September 2024].

[16] Williams B. *The basics of web handling*. https://www.montalvo.com/web-handling-basics/#: :text=Web%20handling%20runs%20and%20controls,machinery%20without%20flaws%20or%20defects [Accessed 3rd September 2024].

[17] Roll-2-Roll Technologies. *Web guides or web guiding systems overview*. https://r2r.tech/articles/web-guides-or-web-guiding-systems-overview [Accessed 3rd September 2024].

[18] Williams B. *Web guiding systems and principles*. https://www.montalvo.com/category/article-library/ [Accessed 3rd September 2024].

[19] Williams B. *What is winding tension?* https://www.montalvo.com/category/article-library/ [Accessed 3rd September 2024].

[20] Seshadri A, Pagilla PR. Optimal web guiding. *Journal of Dynamic Systems Measurement and Control*. 2010;132(1): 011006. https://doi.org/10.1115/1.4000074.

[21] Pedro. *Web guiding fundamentals - normal entry rule*. https://r2r.tech/blog/web-guiding-fundamentals-normal-entry-rule [Accessed 3rd September 2024].

[22] Smith RD. *Guidelines for rolls used in web handling*. https://www.scribd.com/document/475829034/smith-guidelines-for-rolls-used-in-web-handling-presentation [Accessed 28th September 2024].

[23] Tsai SY. *Design and development of a web roll-to-roll testing system with lateral dynamics control of displacement guide*. Master's thesis. Palmerston North, New Zealand: Massey University; 2012.

[24] Pedro. *Web guiding applications and advanced web guiding concepts - center guiding*. https://r2r.tech/blog/web-guiding-applications-and-advanced-web-guiding-concepts-center-guiding [Accessed 5th September 2024].

[25] Seshadri A. *Web guide selection*. https://www.pffc-online.com/web-handling/web-guiding/16525-properly-select-a-web-guide-for-your-operation [Accessed 5th September 2024].

[26] Roll-2-Roll Technologies. *Unwind and rewind guides: design and installation considerations*. https://r2r.tech/articles/unwind-and-rewind-guides-design-and-installation-considerations [Accessed 5th September 2024].

[27] Hopcus K. *What type of web guide do you need?* https://www.maxcess.eu/sites/default/files/documents/files/Fife_GuidingSelection.pdf [Accessed 3rd September 2024].

[28] Williams B. *Web tension control basics*. https://www.montalvo.com/category/article-library/ [Accessed 3rd September 2024].

[29] Yan J, Du X. Web tension and speed control in roll-to-roll systems. In: Voloşencu C, Saghafinia A, Du X, Chakrabarty S (eds.). *Control theory in engineering*. IntechOpen; 2020.

[30] Mishor B. *The importance of tension control*. https://www.montalvo.com/the-importance-of-tension-control/ [Accessed 3rd September 2024].

[31] Williams B. *Dancer or load cells – Which should I use?* https://www.montalvo.com/dancer-or-load-cells-which-should-i-use/ [Accessed 3rd September 2024].

[32] Optimal. *Improving the production process through better web tension control*. https://www.slideshare.net/slideshow/web-tension-control-loadcells-vs-dancer-rollers/13616102 [Accessed 28th September 2024].

[33] Neska M, Majcher A. System for automatic web guiding for roll-to-roll machine working in a start-stop mode. *Solid State Phenomena*. 2015;223: 374–382. https://doi.org/10.4028/www.scientific.net/SSP.223.374.

[34] Mitsubishi Electric Corporation. *Electromagnetic clutches and brakes tenson controller: tension control complete guide*. https://dl.mitsubishielectric.co.jp/dl/fa/document/catalog/clutch/sh-170011eng/sh170011-c.pdf [Accessed 28th September 2024].

[35] Shou W. *Development of an automated nanoparticles spray system for selectively reinforcing polymer composites*. Master's thesis. South Louisiana, United States: University of Louisiana at Lafayette; 2015.

[36] BETE. *Spray nozzles for precision coating*. https://bete.com/application/coating/ [Accessed 28th September 2024].

[37] The Spray Nozzle People Group. *Spray nozzle solutions to industries worldwide*. https://www.spraypeoplegroup.com/brands/spray-nozzle-people/ [Accessed 3rd September 2024].

[38] Codinter. *Spray guns: All about its use, parts and types*. https://www.codinter.com/en/spray-guns-use-parts-types [Accessed 3rd September 2024].

[39] Munson BR, Rothmayer AR, Okiishi TH, Huebsch WW. *Fundamentals of fluid mechanics*. 7th ed. Hoboken, NJ: Wiley; 2013.

[40] Murphy C. *Radiant heating with infrared*. https://www.watlow.com/-/media/documents/training-and-education/stl-radm-89.ashx [Accessed 28th September 2024].

[41] Bastiurea M, Bastiurea M, Andrei G, Dima, D, Murarescu M, Ripa M, et al. Determination of specific heat of polyester composite with graphene and graphite by differential scanning calorimetry. *Tribology in Industry*. 2014;36(4): 419–427.

[42] Lee S. *A study of latent heat of vaporization in aqueous nanofluids*. Doctoral dissertation. Arizona, United States: Arizona State University; 2015. https://core.ac.uk/download/pdf/79581265.pdf [Accessed 28th September 2024].

[43] Klein Tools. *Emissivity chart: Non-metal and metal materials*. https://data.kleintools.com/sites/all/product_assets/documents/brochures/klein/EmissivityChart.pdf. [Accessed 3rd September 2024]

[44] Kosky P, Balmer R, Keat W, Wise G. *Exploring engineering*. 5th ed. Academic Press; 2020.